

LOF and TOP Severe Accident Analysis for PGSFR Using SAS4A Metal Fuel Version Code

S.H. Kang^{a*}, A. Tentner^b, A. Karahan^b, K.L. Lee^a

^aSFR Reactor Design Division, Korea Atomic Energy Research Institute

^bNuclear Engineering Division, Argonne National Laboratory, USA

*Corresponding author: kang@kaeri.re.kr

1. Introduction

PGSFR (Prototype Gen-IV Sodium-cooled Fast Reactor), a pool type sodium-cooled fast reactor with U-10%Zr metallic fuel core and 392.2 MW thermal power capacity, has been under development in KAERI (Korea Atomic Energy Research Institute). PGSFR is composed of two primary pumps, four IHXs (Intermediate Heat eXchangers), four DHXs (Decay Heat eXchangers), two SGs (Steam Generators), two PDHRS (Passive Decay Heat Removal System) and two ADHRS (Active Decay Heat Removal System). The preliminary specific design of PGSFR is completed in 2015. The main feature of PGSFR in safety is from the adoption of the metallic fuel core, leading to inherent reactivity feedback mechanisms and high thermal conductivity [1].

The renewed interest in the analysis of metal fuel core severe accidents in the context of the PGSFR development requires emphasis on the development and validation of the SAS4A metal fuel models that play an important role in describing the accident sequence. A significant metal fuel model development and validation effort has been undertaken at Argonne National Laboratory as part of a collaboration with KAERI. This paper presents results of metal fuel version SAS4A whole core analyses for selected PGSFR postulated severe accidents.

2. SAS4A Metal Fuel Model Developments

The metal-fuel development needs are driven by several important phenomena that occur in metal fuel pins but are not present in the oxide fuel pins: a) the migration of the U-Zr and U-Pu-Zr fuel components during irradiation, which leads to the formation of radial fuel regions with different composition, b) the formation of the fuel-cladding eutectic at the interface between the fuel and cladding, which leads to changes in the local composition of both fuel and cladding, c) the formation of the fuel-cladding eutectic at the outer cladding surface after the cladding failure and fuel ejection in the coolant channel, which affects fuel freezing and cladding ablation, and d) the presence of the in-pin sodium in the molten fuel cavity which can affect the cavity pressure and molten fuel ejection after cladding failure. The changes in the local composition of the fuel and cladding can significantly affect the thermal-physical properties of the materials, including the melting and freezing properties. These changes in turn can affect the timing and magnitude of cladding failure

and material relocation events, and therefore the reactivity feedbacks that determine the core response.

In order to address these metal fuel model extension needs, a significant model development and validation has been undertaken for the SAS4A models, SSCOMP-A (pre-transient metal fuel characterization), DEFORM-5A (transient metal fuel pin mechanics), PINACLE-M (pre-failure in-pin metal fuel relocation) and LEVITATE-M (post-failure metal fuel relocation).

To allow an accurate description of the local fuel composition, the new metal fuel models track twelve fuel components, including: U235, U238, Pu239, Pu240, Pu241, Pu242, Actinides, Fission Products, Lanthanides, Zirconium, Iron, and a Residual component that includes all the mass not included in the previous eleven components. The in-pin sodium and fission gas are also tracked. The changes in the local composition of the fuel have led to significant changes in the reactivity feedback calculation. The reactivity feedback is now calculated by taking into account the axial distribution of each fuel component and its corresponding reactivity worth, while in the previous SAS4A version the fuel composition was assumed to remain unchanged and only one fuel component distribution was used to calculate the reactivity feedback. The impact of the variable fuel composition on reactivity tends to become more pronounced after the cladding failure, because the relocating molten fuel tends to have a composition different from the stationary still-solid fuel [2, 3, 4].

3. PGSFR Modeling

The modeling of the PGSFR core for this analysis is based on the July 16, 2014 core design. The core layout is presented in Fig. 1, consists of 122 driver assemblies (52 in the inner core and 60 in the outer core), 90 reflector assemblies, 102 shield assemblies, and 9 total control assemblies. The PGSFR fuel pin has U-10Zr fuel slug and HT9 cladding. The axial structure of each channel is illustrated in Fig. 2. Zones 1 and 2 represent the lower reflector in the fuel channels. Zone 2 is a 7.2 cm long transition zone from the block-type reflector to the fuel pins. Zone 3 includes the fuel and fission gas plenum, which are 0.978 m and 1.283 m tall, respectively. There are 20 segments in the fuel zone and 5 segments in the fission gas plenum.

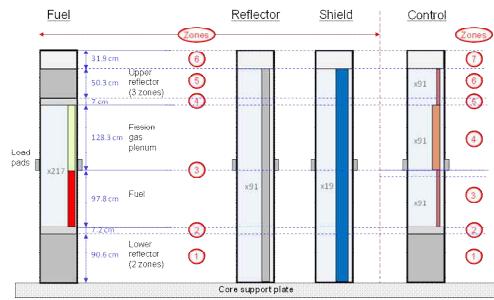
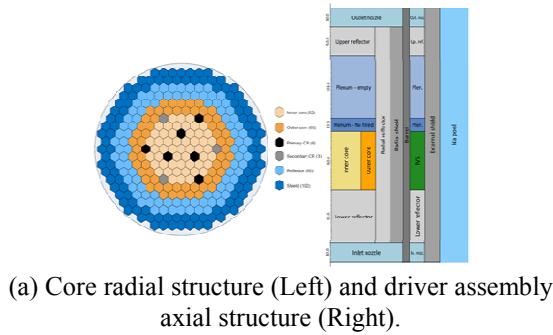


Fig. 1. Core channels Geometry

4. Analysis Results

1. Pre-transient analysis

The pre-transient PGSFR analysis, which defines the initial fuel conditions for the transient calculations, is performed using the SSCOMP-A model. The PGSFR fuel pin has U-10Zr fuel slug and HT9 cladding. A three-batch equilibrium core is modeled with the power highest for the fresh fuel and lowest for the thrice-burned fuel. The cycle length is 602 days. End of Life burnup is 10 at %. The fuel pin in the hot channel for the BOC and EOC conditions has 0.9 at% and 4.7 at% burnup, respectively, and the corresponding core average burnup values are 4.9 at% and 7.6 at%, respectively. The fuel swelling calculated during the pre-transient for the BOC low burnup fuel is small (less than 10 %), whereas the EOC medium burnup fuel is predicted to be fully swollen and in contact with the cladding.

Figs. 2 shows the distribution of the U and Zr weight fractions at the end of EOEC, illustrating the formation of a Zr-rich central region and a Zr-depleted off-center region. The Zr-depleted off-center region extends to the top of the fuel. The distribution of the U weight fraction is illustrated in Fig 3b. The Pu weight fraction is also calculated, but it is not shown due to space limitations. The Pu does not migrate radially during irradiation and differences in the Pu weight fraction tend to be small and due mainly to the changes in the U and Zr weight fractions. The changes in the local fuel composition lead to changes in the fuel thermo-physical properties, including the fuel melting temperature, which are shown in Figs. 3c and 3d. The margin to melting in the Zr-depleted annular region

(Figs. 3d) becomes lower than that in the Zr-rich central region, although the fuel temperature is highest in the central fuel region.

These local fuel composition changes determine the initial conditions for the transient accident analysis and influence significantly the subsequent sequence of events calculated by the SAS4A transient models. The formation of a Zr-depleted off-center zone in the axial region where fuel component relocation occurs favors the formation of an annular molten fuel cavity during the transient, when the power level and fuel temperatures increase. This effect is more pronounced for the higher burnup fuel pin [2, 3, 4].

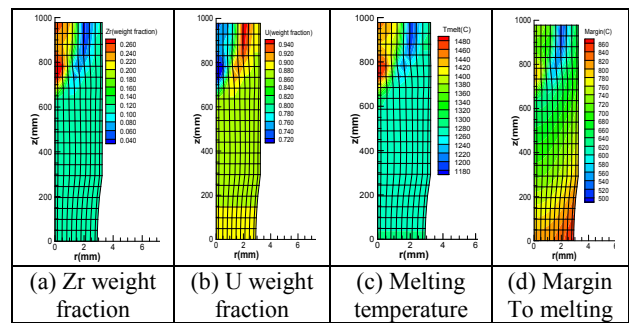


Fig. 2 Fuel status in peak channel

2. Transient analysis

A PGSFR postulated LOF-TOP (Loss Of Flow and Transient Over Power) unprotected transient is analyzed. As transient initiators, rapid main pump impeller torque decrease and reactivity insertion at a rate of 0.02\$/s to the maximum 0.6\$ at 30s are specified. The 0.02\$/s reactivity insertion rate is based on the conservative assumption that one control rod is withdrawn at a rate approximately five times higher than the maximum rate. The hot channel contains 10 fuel assemblies out of a total 112 fuel assemblies.

Figure 3 shows core inlet flowrate and fuel, cladding and coolant temperatures at core outlet. The inlet flowrate decreases due to pump torque reduction. Core outlet temperature increases due to the flow reduction and reactivity insertion, which lead to the onset of coolant boiling at approximately 17s.

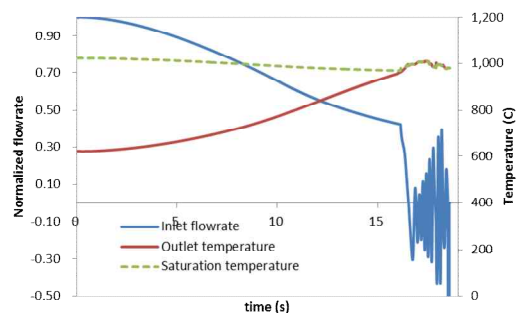


Fig. 3 Coolant flow rate and temperature (EOC)

FIGs. 4a and 4b show the molten fuel cavity evolution in the peak channel at BOC and EOC respectively. An annular molten cavity is formed for the both cases. The annular cavity is due to the off-center region where the fuel margin to melting is lower due to Zr migration. At BOC, PINACLE-M initiates at 18.3s. The molten fuel cavity extends to the top of the fuel and in-pin fuel ejection occurs at 18.5s, prior to the cladding failure. Then cladding failure by hoop stress is predicted at the axial segment 19 at 20.6s and LEVITATE-M is initiated. Although the cladding temperature is close to the molten fuel temperature (approximately 1550 K) it remains below the cladding melting temperature (1700 K). The eutectic penetration, which contributes to cladding failure, is calculated but not shown in the figure.

For the EOC case, PINACLE-M initiates at 17.9s and in-pin fuel ejection occurs at 17.97s. Then LEVITATE-M initiates due to cladding failure by hoop stress at the axial segment 18 at 18.5s. It is noted that although the power level is lower in the EOC case, the plenum fission gas pressure is considerably higher at EOC, causing the EOC cladding failure to occur 2.1 s earlier than the BOC cladding failure.

The molten cavity size for the BOC case prior to onset of in-pin molten fuel motion is predicted to be significantly larger than that predicted for the EOC case. This is due to higher power levels and fuel temperatures at BOC, caused by different characteristics of the low burnup (BOC) and medium burnup (EOC) fuels. The negative reactivity feedbacks during overheating due to solid fuel axial expansion and Doppler are smaller for the BOC fuel. The BOC solid fuel is not yet in hard contact with the cladding and can expand both radially and axially, whereas the higher burnup EOC fuel is fully swollen prior to the transient and is forced to expand only axially. This causes the EOC axial fuel expansion to be larger than at BOC bringing in more negative reactivity and leading to a lower EOC power level.

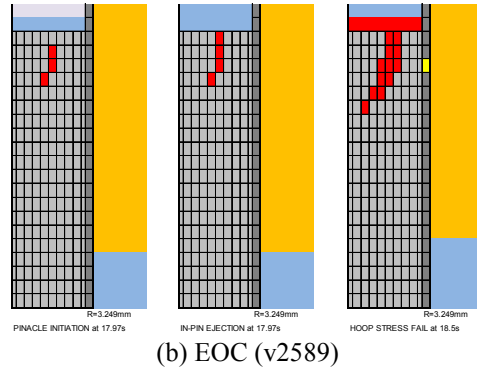
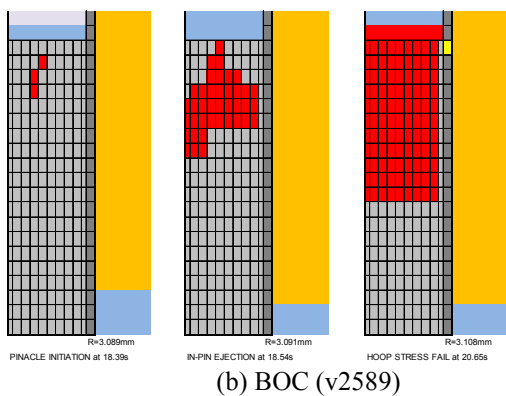


Fig. 4 Molten fuel cavity evolution in peak channel

FIG 5 shows void fraction and voided node in peak channel, and FIG. 6 shows reactivity component history during the transient. Significant coolant boiling and core voiding occurs in both BOC and EOC cases prior to cladding failure. At the time of cladding failure the lead channel core region is approximately 50% voided for the BOC case and 45% voided for the EOC case. Due to the overall negative void reactivity of the PGSRF core the coolant reactivity shown on Figure 6 is negative in both cases.

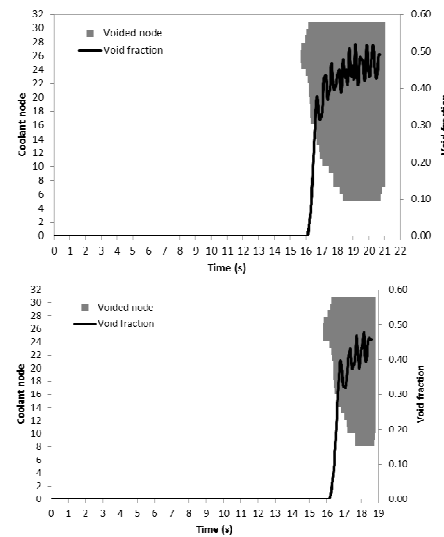
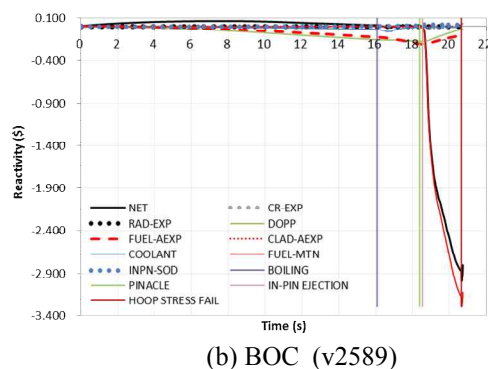
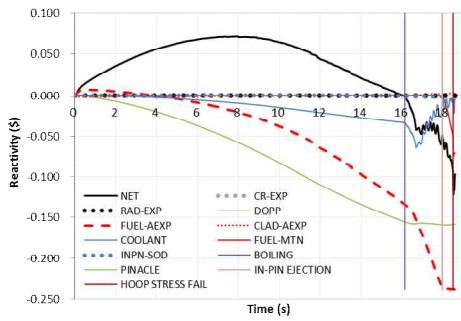


Fig. 5. Void fraction and voided node during transient for LOF-TOP





(b) EOC (v2589)

Fig. 6. Reactivity during transient for LOF-TOP

FIG. 7 shows power and net reactivity during the transient. The relative power at the time of clad failure is approximately $P=0.2P_0$ at BOC and $1.00P_0$ at EOC.

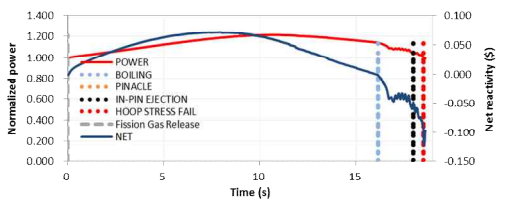
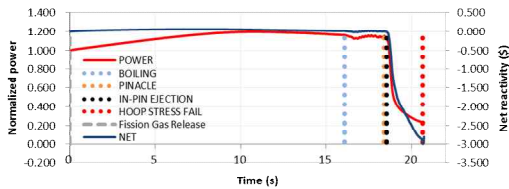
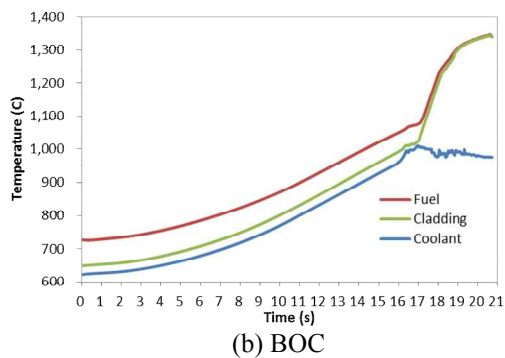
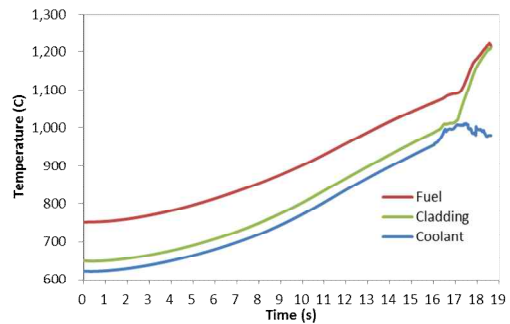


Fig. 7. Net reactivity and power history during transient for LOF-TOP

Figs 8 shows maximum temperatures of fuel, cladding and coolant at the peak channel. The fuel and cladding temperatures are vales at the radially innermost nodes at the fuel top.



(b) BOC



(b) EOC

Fig. 8. Fuel, cladding and coolant temperature (v2589)

5. Conclusion

Whole core analyses for selected PGSFR postulated accidents are performed using newly developed metal fuel version SAS4A code, and core behavior and reactivity feedback during initial phase severe accident are investigated.

ENDNOTES

This study was supported by the Ministry of Science, ICT, and Future Planning of Korea. This work was supported by the National Research Foundation of Korea (NRF) grant funded by the Korean government MSIP (No. 2012M2A8A2025634 and 2011-0031933). And this work was performed in and supported by a collaboration between KAERI and ANL under an interagency agreement.

REFERENCES

- [1] S.H. KANG et al., "Safety Analyses of Design Basis and Design Extended Condition Events for the PGSFR," Transactions of the American Nuclear Society, Vol. 114, New Orleans, Louisiana, June 12–16, (2016).
- [2] A. TENTNER et al., "SAS4A Model Development for the Analysis of Postulated Severe Accidents in Metal Fuel Sodium Fast Reactors, Transactions of the American Nuclear Society," Transactions of the American Nuclear Society, Vol. 115, Las Vegas, NV, November 6–10, (2016).
- [3] A. KARAHAN et al., "Validation of Advanced In-Pin Metallic Fuel Models of SAS4A," Transactions of the American Nuclear Society," Transactions of the American Nuclear Society, Vol. 115, Las Vegas, NV, November 6–10, (2016).
- [4] A. TENTNER et al., "Advances in the Development of the SAS4A Code Metallic Fuel Models for the Analysis of Prototype Gen-IV Sodium-cooled Fast Reactor Postulated Severe Accidents," International Conference on Fast Reactors and Related Fuel Cycles: Next Generation Nuclear Systems for Sustainable Development (FR17), Yekaterinburg, Russian Federation, June 26–29, (2017).